Egypt. J. Chem. **Vol. 67**, No. 1 pp. 319 - 331 (2024)

Egyptian Journal of Chemistry

http://ejchem.journals.ekb.eg/

Synthesis, chemical characterization, and anti-proliferative action of 1,2,4-triazole N-glycoside derivatives

Hala E.M. Tolan[1], Asmaa M Fahim[2] *and Eman H. I. Ismael[3]*

[1]*Department of Photochemistry, National Research Centre, Dokki, P.O. Box.12622, Cairo, Egypt.*

[2]*Department of Green Chemistry, National Research Center, Dokki, P.O. Box.12622, Cairo, Egypt.*

[3]*Department of Organometallic and Organometalloid Chemistry, National Research Centre, Dokki, P.O. Box.12622, Cairo, Egypt*

Abstract

In this study, we have reacted the mercapto-N-phenyl-1,2,4-triazolothiazolo derivative **1a** with acetylated bromogalactose**2a** to give the new O-acetylated N-phenyl-1,2,4-triazolo thiazolotetrahydropyranethioglycoside derivative **3a** in a good yield. Treatment of the acetylated thioglycoside derivative **3a** with ammonia solution in methanol resulted in de-acetylation where the corresponding free hydroxyl-tetrahydropyranethioglycoside derivative **4a** has been formed. Similarly, reaction of the -N-amino-1,2,4- triazolothiazolo derivative **1b** with a five-membered ring glycoside derivative ,namely, acetylated bromo ribose **2b** gave the corresponding new O-acetylated N-amino-1,2,4-triazolothiazolo- tetrahydrofuranethioglycoside derivative **3b.** Hydrolysis ofcompound **3b** with ammonia in methanol yielded the corresponding free hydroxyltetrahydrofuranethioglycoside derivative **4b.** Structures of the new products were elucidated with compatible micro analytical and spectroscopic (FT-IR, 1H-NMR, 13C-NMR) measurements. The new synthesized 1,2,4-triazole glycoside derivatives **3a,b** and **4a,b** were found to exhibit anticancer activity *invitro* against a number of human cancer cell lines, including MCF-7 and HCT-116. The structural analysis of the KSHV thymidylate synthase (PDB ID: 5h38) and the crystal structure of the Ternary Complex of KRIT1 bound to the Rap1 GTPase and the Heart of Glass (HEG1) cytoplasmic tail (PDB ID: 4hdq) were both used to determine the potential interactions of glycosyltriazoles. Additionally, the 1,2,4-triazole N-glycosides **3a**, **3b**, **4a**, and **4b** were proven to be stable by employing the DFT/B3LYP/6-31G(d) basis set to explore and determine the physical descriptors of the existence of the acetyl and hydroxy groups of the glycoside ring using FMO.

Keywords:1,2,4-triazole-N-glycosides; Docking simulation; Anti-proliferative action theoretical research.

1. Introduction

A glycosidic connection connects the 1,2,4-triazole ring to a sugar moiety to form a class of substances known as 1,2,4-triazole-N-glycosides. These compounds have drawn a lot of interest in the domains of medicinal chemistry and chemical biology because of their potential biological activity and variety of uses. [1-3]. To make 1,2,4-triazole-N-glycosides, click chemistry, or the copper(I)-catalyzedazide-alkyne cycloaddition process, is widely utilized. The 1,2,4-triazole ring can be successfully created by joining an azide and an alkyne functional group. Additionally, it is used in biological activities like antimicrobial, antiviral, anticancer, and antitumor properties. The union of the sugar moiety with the 1,2,4-triazole ring can lead to increased activity, improved stability, and altered pharmacokinetic properties compared to the parent compound.[3-11]. Additionally, the presence of the sugar moiety permits potential interactions with biological targets, such as enzymes, receptors, and transporters, as well as having an impact on the solubility and bioavailability of the compound. There are several glycoside medications in her that are utilized as anticancer and antiviral medications, such as Vidarabine(I).[12], While gemcitabine (II) is used to treat various cancers, including bladder cancer [13-15] and breast cancer and Tobramycin(III) which used as antibiotic for eye to treat bacterial infections for eye [16-18]as displayed in **Figure.1.**

*Corresponding author e-mail: emanhamed125@yahoo.com

Receive Date: 14 June 2023, Revise Date: 19 July 2023, Accept Date: 23 July 2023

DOI: 10.21608/ejchem.2023.217561.8139

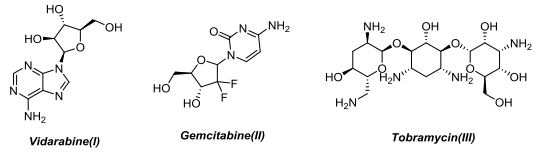

Figure.1: Some drugs contain different glycoside moieties

In this study, we created novel 1, 2, 4-triazole N-glycosides by combining amino triazole with acetylated bromogalactose and acetylated bromo ribose to produce the thioglycosides**3a** and **3b**, which readily dehydrate in the presence of ammonia to produce hydrated aminothiazoleglycoside derivatives **4a** and **4b**. Along with these glycosides, MCF-7 and HCT-116 colon and breast cancer cell lines, respectively, showed that the glycosides have anticancer action. These findings were verified using molecular docking simulation, the DFT/B3LYP/6-31(G) basis set, and the physical descriptors and FMO, which also verified the biological inquiry.

2. Results and Discussion

2.1.Chemistry:

When hydrazide was treated with phenyl isothiocyanate, the corresponding aryl substituted thiosemicarbazide derivative was formed in large quantities; when it heterocyclized in sodium hydroxide solution, it created the 1,2,4-triazolethiol as in literature. [3]. The related 1,2,4-triazole thioglycosides were created by glycolyzing the S-triazole derivative with acetylated glycosyl halide of the galactose and ribose moieties. In the current study, the triazole derivative **1a** was used to produce the thioglycoside molecule, namely (3*S*,4*R*,5*R*)-2-(acetoxymethyl)-6-((5-(5-oxo-1-(thiazol-2-yl)-4-(thiazol-2-ylamino)-2,5-dihydro-1*H*-pyrrol-3-yl)-4-phenyl-4*H*-1,2,4-triazol-3-yl)thio)tetrahydro-2*H*-pyran-3,4,5-triyl triacetate**(3a)** by reacting with acetylated bromogalactose**2a** in acetone. The structure of these glycosyls is clarified by IR and ^{1}H NMR. Compound 3a's IR spectrum revealed characteristic absorption bands at 3211 and 1728 cm^{-1} corresponding to NH and C=O groups, respectively, and its ^{1}H NMR revealed signals at 1.95-2.01 ppm referring to CH_3 groups as well as the protons of sugar and aromatic rings. It also revealed a signal at 9.12 ppm corresponding to NH group. Utilizing methanol and an ammonia solution, the thioglycoside molecule **3a** was hydrated to produce the hydroxyl compound, namely 4-(4-phenyl-5-((3*S*,4*R*,5*R*)-3,4,5-trihydroxy-6-(hydroxymethyl)tetrahydro-2*H*-pyran-2-ylthio)-4*H*-1,2,4-triazol-3-yl)-1-(thiazol-2-yl)-3-(thiazol-2-ylamino)-1*H*-pyrrol-2(5*H*)-one (**4a**), its ^{1}H NMR revealed signals of OH groups at various regions at 4.42, 4.69, and 4.90 ppm in addition to the protons of the glycosyl and aromatic rings in the compound. Its IR spectrum revealed absorption bands at 3354 and 3240 cm^{-1} according to OH and NH groups, respectively as shown in **Scheme 1**. Contrarily, the acetylated bromo ribose **2b** was reacted with the triazole derivative **1b**, which was produced from hydrazide with hydrochloric acid as mentioned in the literature to produce the glycosyl molecule, namely (2*R*,3*R*,4*S*,5*R*)-2-(acetoxymethyl)-5-(4-amino-5-(5-oxo-1-(thiazol-2-yl)-4-(thiazol-2-ylamino)-2,5-dihydro-1*H*-pyrrol-3-yl)-4*H*-1,2,4-triazol-3-ylthio)tetrahydrofuran-3,4-diyldiacetate (**3b**); the latter compound's characteristic absorption bands at 3208 and 1705 cm^{-1}, which correspond to NH and C=N groups, were seen in the compound's infrared spectra; Its ^{1}H NMR displayed signals for the methyl groups at 1.51-1.82 ppm as well as for the other protons in the molecule and a broad signal for the NH group at 9.29 ppm. Utilizing a solution of methanol and ammonia to convert methyl groups to hydroxyl groups, glycosyl**3b** was deacetylated to produce compound 4-(4-amino-5-((2*R*,3*S*,4*R*,5*R*)-3,4-dihydroxy-5-(hydroxymethyl) tetrahydro furan-2-ylthio)-4*H*-1,2,4-triazol-3-yl)-1-(thiazol-2-yl)-3-(thiazol-2-ylamino)-1*H*-pyrrol-2(5*H*)-one (**4b**). Its ^{1}H NMR spectrum revealed signals at 4.89, 5.22, and 6.89 ppm corresponding to OH groups, as well as the protons of the sugar in this compound's structure, as shown in **Scheme 2.** The IR spectrum of this formed compound revealed the presence of hydroxyl groups in its region instead of acetyl groups, and showed absorption bands at 3460 cm^{-1} characteristics to OH groups.

3.Biological evaluation:

3.1. Anti-tumor Activity:

In vitro anticancer efficiency against the tumor cells HCT-116 and MCF-7: Using the sulforhodamine B (SRB) colorimetric assay, Skehan et al. evaluated the anti-proliferative activity of the 1,2,4-triazole acetylated N-glycoside derivatives 3a, 3b, 4a, and 4b against two human cancer cell lines, including the HCT-116 colon cancer cell lineand MCF-7 breast cancer cell line[19, 20]. Doxorubicin served as a reference cytotoxic substance in the experiments. Growth inhibitory concentration (IC50) values were used to express the results, which show the drug

concentrations needed to result in a 50% inhibition of cell growth after 72 hours of incubation compared to untreated controls (Table 1).

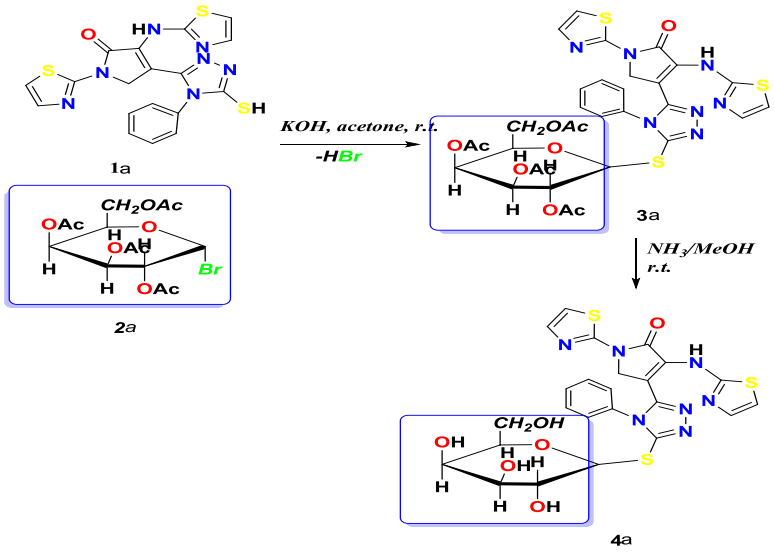

Scheme 1: Reaction of amino triazole with Bromogalactose derivatives

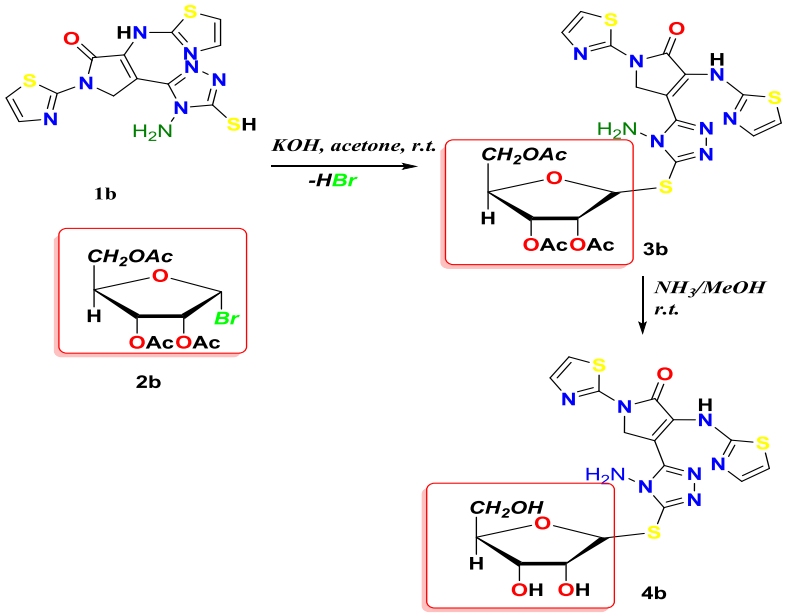

Scheme 2: Reaction of amino triazole with Bromo Ribose derivatives

According to the discovered results, the produced compounds showed outstanding growth inhibitory activity against the examined cancer cell lines comparable to the noticed activities for the reference medication doxorubicin. Studies on the cytotoxic activity against the two cell lines revealed that they are very comparable in terms of their receptivity to

the effects of the chemicals under test.[18]. The obtained results were interpreted to mean that the synthesized triazole glycosides had outstanding growth inhibitory action against the tested cancer cell lines, HCT-116 and MCF-7, because these cells were more sensitive to the effects of the tested compounds [43–45]. For HCT-116, compounds 3a, 3b, 4a, and 4b showed IC50 values of 23.3 ± 2.7, 23.4 ± 3.1, 38.7 ± 4.1, and 27.0 ± 2.6 µg/ml, respectively, whereas MCF-7 showed IC50 values of 22.9 ± 2.7, 22.0 ± 2.3, 21.0 ± 2.1, and 17.1 ± 1.8 µg/ml, respectively, against doxorubicin. Compound **4b** is obviously more effective against MCF-7 cell lines as it is of higher activity comparable with doxorubicin and **4a** showed moderate activity. Furthermore, the glycosides **3a**, **3b**,**4a** and **4b** have the less activity potent with HCT-116 cell line compared with IC50 of doxorubicin (12.3 ± 1.9µg/ml).

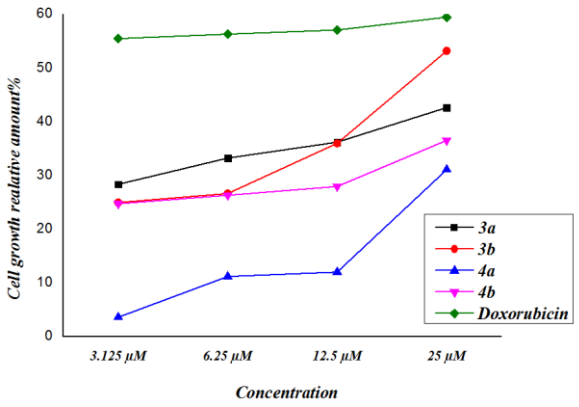

(A)HCT-116

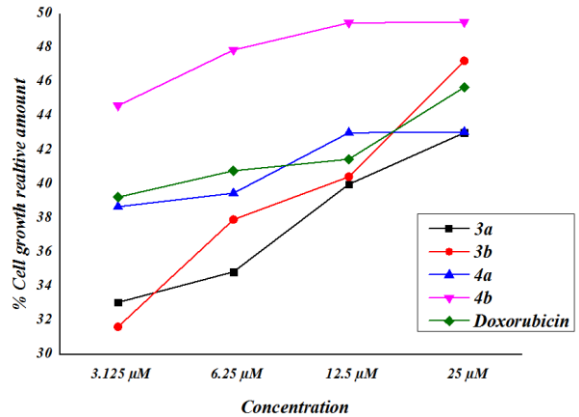

(B) MCF-7

Figure.2. Plot concentration of tumor cells for 48 h in the occurrence of aggregate concentrations of compounds **3a** ,**3b** , **4a** and **4b** , in evaluation to Doxorubicin against HCT-116 and MCF-7 tumor cells

Table 1: *In vitro* cytotoxic activities of the newly synthesized compounds against HCT-116 and MCF-7 cell lines.

Compound Code	**IC_{50} (µM) ± SD**	
	HCT-116	**MCF-7**
3a	23.3 ± 2.7	22.9 ± 2.7
3b	23.4 ± 3.1	22.0 ± 2.3
4a	38.7 ± 4.1	21.0 ± 2.1
4b	27.0 ± 2.6	17.1 ± 1.8
Doxorubicin	12.3 ± 1.9	20.5 ± 2.1

[a]IC_{50} values are the mean ± S.D. of three separate experiments.

3.2. Structural Activity Relationship(SAR):

It's crucial to remember that sugars' SAR can be quite complex and context-dependent since a variety of factors, including stereochemistry, substituent groups, and interactions with certain receptors or enzymes, can affect how they behave. Additionally, because there are numerous six-carbon and five-carbon sugars with various modifications and derivatives, the SAR can change for various glycoses. We noticed that reactivity of five and six membered glycoside due to their low angle, eclipsing strain and presence of heteroatom in the glycoside ring which inhibit the tumor cell comparable with Doxorubicin drug according the Huckle rule with if a cyclic, planar molecule has 4n+2 π electrons, it is considered aromatic and refer to stability of six cyclic sugar but the five cyclic sugar more active than six membered ring and presence of OH, NH_2 and OAc increase intramolecular hydrogen bond interactions.

3.3. Docking simulation:

The docking investigation of compounds **3a**, **3b**, **4a** and **4b** with flexible docking of the compounds was talented in the crystallographic structure of the Ternary Complex of KRIT1 bound to both the Rap1 GTPase and the Heart of Glass (HEG1) cytoplasmic tail PDBID:(4hdq)[21] and Structural analysis of KSHV thymidylate synthase PDBID:5H38 using MOE docking program [22]as displayed in **Figure.3** and **Table.2.** Docking interaction with Crystal Structure of the Ternary Complex of KRIT1 bound to both the Rap1 GTPase and the Heart of Glass (HEG1) cytoplasmic tail (PDB ID: 4hdq), where its

KRIT1 protein contains three NPX(Y/F) motifs, four ankyrin repeats, and a C-terminal FERM domain. It was first identified as a Rap1-binding protein by yeast two-hybrid screen. The crystal structure of the KRIT1 FERM domain in conjunction with Rap1 reveals that it interacts with the F1 lobe of KRIT1 in a manner similar to a GTPase-ubiquitin fold interaction, but it also binds the F2 lobe through a unique interaction. KRIT1 binds to Rap1 with a 10-fold greater affinity than HRas, but it is unclear how this exceptional Rap1-specificity is achieved. The Ternary Complex of KRIT1 linked to the Rap1 GTPase and the Heart of Glass (HEG1) cytoplasmic tail may be seen in the crystal structure (PDB:4hdq) [23]interact with compounds **3a**, **3b** , **4a** and **4b** containing the glycoside moieties, respectively. The hydrogen bond interaction with excellent confirmation interaction energy of compound 4b with energy affinity -12.235(kcal/mol), distance 2.67, 2.6, 2.93 Å and interaction protein's (Asn 496, Thr 695, Lys 713, Thr 641, Gly 642, Gln 643, Thr 712, Phe 645, His 711),while the energy of compound **4a** was -11.621(kcal/mol) and bond distance 2.98 Å with different protein's (Lys 720, Met 723, Trp 688, Met 687, Leu 690, Asp 694) and the compounds **3a**, **3b** before hydration showed the less binding affinity with-10.321 and -10.921; respectively as elucidated in Table.**2** and shown in Figure.**3** and more correlated with experimental results[24, 25].

Table 2. The molecular docking of glycoside derivatives with different proteins:

Rap1 GTPase and the Heart of Glass (HEG1) cytoplasmic tail PDBID: 4hdq				***Structural analysis of KSHV thymidylate synthase PDBID:5H38***			
	Enerey affinity(kcal/mol)	*Distance(Å)*	*Amino acids*		*Energy affinity (kcal/mol)*	*Distance(Å)*	*Amino acids*
3a	-10.321	2.85Å	Gln 696, Asp 692, Cys 696, His 711, Gln 689, Thr 695, Thr 693	***3a***	-10.231	3.07,2.63, 1.47Å	Glu 63, Arg 67, Arg 59, Gln 86
3b	-10.921	2.78Å	His 711, Gln 643, Asn 496, Lys 713, Thr 712, Gly 642	***3b***	-10.521	1.35, 2.5, 2.66Å	Glu 313, Arg 164, Lys 193, Asp 190
4a	-11.621	2.98Å	Lys 720, Met 723, Trp 688, Met 687, Leu 690, Asp 694	***4a***	-9.621	2.45Å	Ala 228, Glu 231, Asp 229, Arg 92, Tyr 226, Arg 88, Glu 271
4b	-12.235	2.78Å	Asn 496, Thr 695,	***4b***	-8.325	2.66, 2.5, 1.35Å	Gln 313, Lys 193,

			Lys 713, Thr 641, Gly 642, Gln 643, Thr 712, Phe 645, His 711				Arg 164, Ser 186, Asp 183

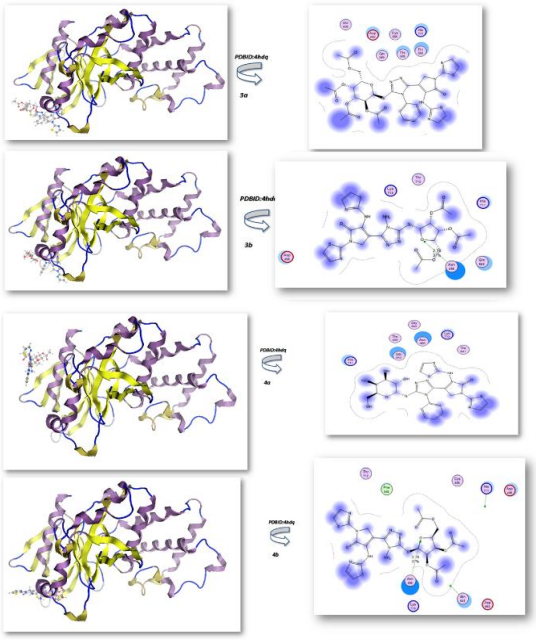

(A) 4hdq

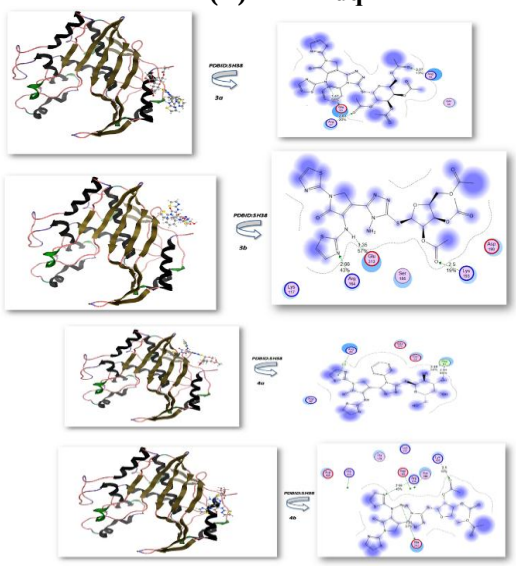

(B)5H38

Figure.3. Docking stimulation investigation of synthesized compounds with PDBID:4hdq and PDBID:5H38

Interaction with docking KSHV (Kaposi's sarcoma-related herpesvirus) is an oncovirus that is associated with Kaposi's sarcoma in AIDS patients, primary effusion lymphoma, and other kinds of multi-centric Castleman's infections. Structural investigation of KSHV thymidylate synthase (PDB ID: 5h38). The useless thymidylate synthase (kTS) encoded by KSHV is 70% categorically similar to human TS (hTS). Thymidylate synthase (TS) has been characterized in its three-dimensional configurations for many different organisms, with the exception of E. coli, Lactobacilluscasei, Bacillus subtilis, rats, and humans. A molecular modelling research was conducted in an effort to explain the cytotoxic activity profile displayed by the synthesized drugs. The synthesized compounds were subjected to a conformational search using an implicit solvent model, which was followed by a quantum-mechanical (QM) technique for fine-tuning the geometry of local minima. The compounds were then flexible docked in the crystal structure of the KSHV thymidylate synthase with a native sulfonamide obtained from the Protein Data Bank (PDB ID: 5h38) to assess their potential ability to bind in the active pocket of KSHV as a potential molecular target. Our glycosides were found to bind to KSHV in poses that resembled co-crystallized ligands. The compound **3a** and **3b** showed the most potent activity with binding energy -10.231 and -10.521; respectively and its shortage bond length 3.07,2.63, 1.47 ,2.89, 2.84 Å with different amino acids (Glu 63, Arg 67, Arg 59, Gln 86)(Arg 88, Glu 271, Glu 53, Pro 51, Arg 92) and 4a, 4b showed -9.621 and -8.325kcal/mol, with length 2.45, 1.8, 2.74,2.44 Å, its interaction NH_2, C=O, OH which increased their stabilities[26, 27].

4. Computational Calculation's:

4.1. Physical descriptors of synthesized compounds:

In this studies , we optimized the glycoside derivatives utilized Gaussian(09)[28-30] through DFT/B3LYP/6-311(G) basis set. Moreover, the physical characteristics used in the optimization of molecular structures of compounds 3a,3b,4a,4b wereconcerning (σ) absolute softness[31], (χ) electronegativities[32], (ΔN_{max}) electronic

charge[33], (η) absolute hardness, (ω)[34] global electrophilicity[35], (S) global softness[36], and (Pi) chemical potential[37], from the equations [**1-8**] which were scheduled in **Table .3** and **Figure.4**

$\Delta E = E_{LUMO} - E_{HOMO}$	**[1]**	$\chi = \frac{-(E_{HOMO}+E_{LUMO})}{2}$	**[2]**
$\eta = \frac{(E_{LUMO}-E_{HOMO})}{2}$	**[3]**	σ=1/ η	**[4]**
Pi=-X	**[5]**	S =1/2 η	**[6]**
ω= $Pi^2/2$	**[7]**	ΔN max=- Pi/ η	**[8]**

The optimized structures showed non planarity of these glycoside due to presence of glycoside moiety which make more electrostatic hydrogen interaction which change of the confirmation of chain structure, The potential activities presented in the precursor of compounds 3b, 4b due to presence of amino group which showed increased activity and more stability rather than the glycoside 3a and 4a in which the electrons are restricted in the ring and make more hydrogen bonding interaction. The two p-isoelectronic structures of compounds 4a and 4b utilizing DFT/B3LYP/6-31G(d)[38-41] with the same stability, even though the DFT/B3LYP/6-31G(d) seems to be more stable for compound 4a than 4b through (842.73702eV) (≈ 19433.972kcal/mol). The dipole moment of compound 4b showed that μ of DFT/B3LYP/6-31G(d)> μ of DFT/B3LYP/6-31G(d) for 4a through 1.7713 as displayed in Table 3 due to presence of OH group which gave its easily charge separation than 4a, while the energy of 3a and 4a showed less than aminatedglycose due to absence of amino group and difference between them in presence of acylated and deacylated sugar showed (2437.869e V)(56218.58kcal/mol) and difference in dipole moment with 1.0002 Debye which can be easily make charge separation[42].

The energy gap of 1,2,4 -triazole glycoside derivatives **3a, 3b, 4a and 4b** possessing the glycoside ring and its structural analogue incorporating the triazole moiety utilizing DFT/B3LYP/6-31(G)-dbasis set showed approximately same band energy gap with 3.3266181, 3.7279892, 3.78649414, 3.757377728 eV, respectively. And showed mostly the distribution of electrons on the triazole ring which increased its stabilities which attached to glycoside ring and mainly oriented of atom which make hydrogen interaction. Moreover, the (χ) absolute electronegativity's which showed affinity of atom interaction with mutual pair of electrons and they showed approximately same value with 3.990 , 3.761,3.916, 3.699 eV; respectively which can easily make more interaction with each other's and the chemical hardness η(eV) indicates the extent resistance of change of electron cloud density in the system and showed same value with 1.663,1.864, 1.893, 1.880 e V, and the chemical potential Pi showed its ability to react and absorb more energy in different temperature range and they same which can easily absorb more energy with same sequence, The (ΔNmax) electronic charge for **3a** showed high value with 2.39927 e V due to presence of Acetyl group to interact again[43] , while the same value in **3b** and **4a** and then decresaed again **4b** with 1.9675531 e V [23, 44-46]as dsipalyed in **Table.3.**

5. Experimental:

5.1.Instrument:

The Gallenkamp melting point apparatus was used for measuring melting points. Moreover, Shimadzu FT-IR 8101 PC infrared spectrophotometer recorded the IR spectra. The 1H NMR and 13C NMR spectra were determined in DMSO-d6 at 300 MHz on a Varian Mercury VX 300 NMR spectrometer (1Hat 300 MHz,13Cat75MHz) exhausting trimethylsilane as an internal typical. Shimadzu GCMS-QP 1000 EX mass spectrometer at 70 eV was used to measure mass spectra. Elemental analyses were approved out at the MicroanalyticalCenter of Cairo University, Giza Egypt.

5.2.Synthesis of 1,2,4-triazole acetylated S-glycosides derivatives:

5.2.1.General procedure:

A solution of acetylated glycopyranosyl bromide (0.1 mol) (galactose or ribose) in acetone (30 ml) was added to a well stirred mixture of triazolederivative**1**(10 mmol), potassium hydroxide (10 mmol) and water (2 ml). The resulting mixture was stirred at room temperature for 4 h followed through filtration of the fine powder and evaporation of the solvent under reduced pressure. The residue was washed with distilled water then extracted with ethyl acetate. The organic layer was washed with water, dried and the solvent was evaporated to afford compounds **3a** and **3b**, respectively.

*(3S,4R,5R)-2-(acetoxymethyl)-6-((5-(5-oxo-1-(thiazol-2-yl)-4-(thiazol-2-ylamino)-2,5-dihydro-1H-pyrrol-3-yl)-4-phenyl-4H-1,2,4-triazol-3-yl)thio)tetrahydro-2H-pyran-3,4,5-triyl triacetate***(3a):**

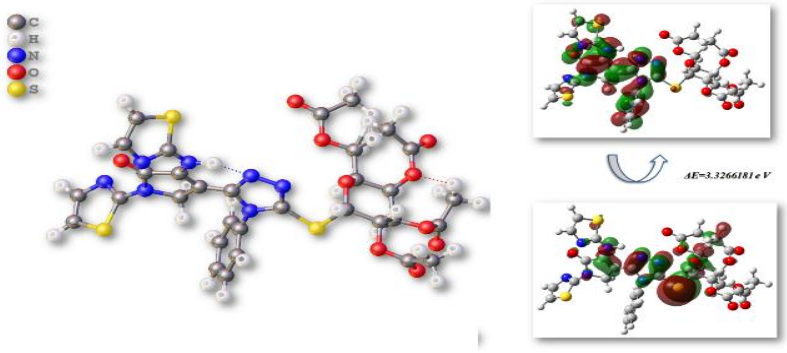

Compound 3a

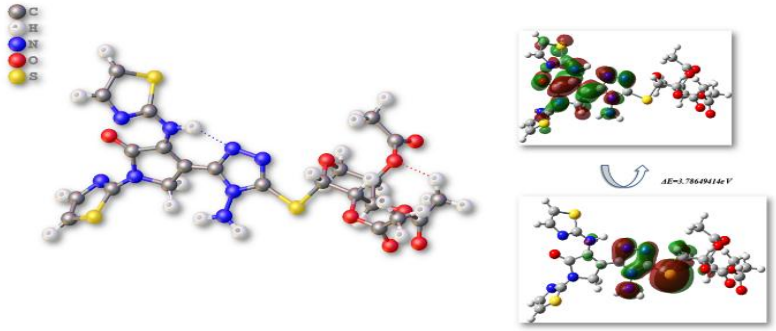

Compound 3b

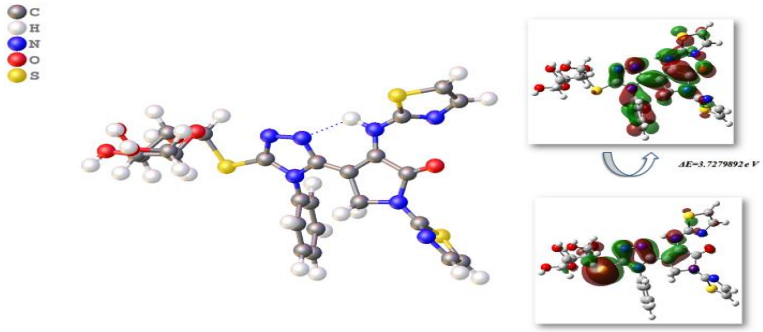

Compound 4a

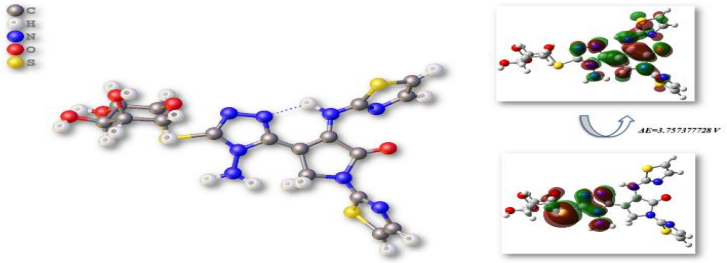

Compound 4b

Figure 4. Calculated structures with HOMO-LUMO energy gap of synthesized compounds.

Table.3. Ground state energies of compound **3a,3b,4a,4b utilizing** DFT/B3LYP/6-311G(d) with their physical parameters:

DFT/B3LYP/6-311G(d)				
	3a	**3b**	**4a**	**4b**
E_T **(au)**	-5321.01	-5231.42	-6452.22	-6421.25
E_{HOMO} **(eV)**	-5.65293	-5.6249098	-5.80913236	-5.5792895
E_{LUMO} **(e v)**	-2.326319	-1.8969206	-2.0226382	-1.81855122
E_g **(eV)**	3.3266181	3.7279892	3.78649414	3.757377728
μ (D)	5.353	6.3532	7.464	9.2353
χ (eV)	3.990	3.761	3.916	3.699
η(eV)	1.663	1.864	1.893	1.880
σ(eV)	0.601	0.536	0.528	0.532
Pi(eV)	-3.990	-3.761	-3.916	-3.699
S(eV)	0.301	0.268	0.264	0.266
ω(eV)	4.785	3.794	4.050	3.638
ΔN max	2.39927	2.0177038	2.0686740	1.9675531

Yield: 62%; m.p. 166-168^{o}C; IR (KBr) cm^{-1}, ν: 3211 (NH), 1728(C=O);^{1}H NMR (DMSO-d$_6$) δ/ppm: 1.95, 1.96, 1.98, 2.01 (4s, 12H, 4CH$_3$), 3.58-3.62 (m, 1H, H-5′), 3.83-3.94 (m, 3H, H-6″, N-CH$_2$), 4.14 (dd, 1H, J = 3.8, 10.2 Hz, H-6′), 4.57 (dd, 1H, J =8.4, 6.4 Hz, H-4′), 5.18 (dd, 1H, J = 9.8, 7.8 Hz, H-2′), 5.34 (d, 1H, J = 9.8 Hz, H-1′), 5.61 (t, 1H, J = 7.8 Hz, H-3′), 6.91-7.13 (m, 3H, 2S-CH=, Ar-H); 7.21-7.33 (m, 3H, N-CH=, Ar-H), 7.40-7,48 (m, 3H. Ar-H), 9.12 (br, 1H, NH).^{13}C NMR (DMSO-d$_6$, δ ppm): 18.7, 19.2, 20.4, 23.2 (4CH$_3$), 58.1 (CH$_2$), 65.1 (C-6′), 66.9 (C-4′), 71.4 (C-3′), 76.6 (C-2′), 80.8 (C-5′), 94.2 (C-1′), 105.7, 110.2, 117.8, 131.1, 115.2, 119.1, 120.2, 123.5, 128.1, 131.9, 135.7, 138.5, 145.9, 154.2, 157.4, 166.1 (thiazole-C, pyrrole-C, triazole-C), 167.5, 168.9, 170.8, 171.5, 174.6 (5C=O). Anal. Cald. For $C_{32}H_{31}N_7O_{10}S_3$ (769.13): C, 49.93; H, 4.06; N, 12.74. Found: C, 49.95; H, 4.08; N, 12.77 %.

(2R,3R,4S,5R)-2-(acetoxymethyl)-5-(4-amino-5-(5-oxo-1-(thiazol-2-yl)-4-(thiazol-2-ylamino)-2,5-dihydro-1H-pyrrol-3-yl)-4H-1,2,4-triazol-3-ylthio)tetrahydrofuran-3,4-diyldiacetate (**3b**):Yield: 70%; m.p. 141-143^{o}C; IR (KBr) cm^{-1}, ν: 3208(NH), 1705 (C=O);^{1}H NMR (DMSO-d$_6$) δ/ppm: 1.51, 1.53, 1.81 (3s, 9H, 3CH$_3$), 3.57-3.76 (m, 3H, H-5″ and N-CH$_2$), 4.12 (dd, 1H, J = 6.7, 9.3 Hz, H-5′), 4.13 (dd, 1H, J = 7.7, 9.8 Hz, H-4′), 5.31 (dd, 1H, J =9.5, 10.2 Hz, H-2′), 5.41 (brs, 2H, NH$_2$), 5.52 (d, 1H, J = 11.2 Hz, H-1′), 5.69 (dd, 1H, J = 8.4, 6.8 Hz, H-3′), 6.52-6.89 (m, 2H, 2S-CH=); 7.28-7.67 (m, 2H, 2N-CH=), 9.29 (brs, 1H, NH). ^{13} C NMR (DMSO-d$_6$, δ ppm) : 21.5, 22.2, 24.4, 26.1 (4CH$_3$), 52.9 (CH$_2$), 63.9 (C-4′), 69.7 (C-3′), 71.8, (C-2′), 78.9 (C-5′), 86.1 (C-1′), 90.7, 96.2, 98.7, 101.1, 114.5, 132.9, 144.5, 152.6, 161.8(thiazole-C, pyrrole-C, triazole-C), 163.5,166.3, 169.8, 172.5, 176.1 (5C=O). Anal. Cald. For $C_{23}H_{24}N_8O_8S_3$(636.09): C, 43.39; H, 3.80; N, 17.60. Found: C, 43.44; H, 3.88; N, 17.67 %.

5.3. Preparation of deacetylatedS-glycosides 4a,b:

A solution of the acetylated glycoside derivatives (galactose or ribose)**3a**or **3b** (0.5 g) in saturated methanolic ammonia (20 mL) was stirred at room temperature for 7 h. After completion of the deacetylation process (TLC: petroleum ether/hexane, 2:1), the solvent was evaporated under reduced pressure at 40 °C and the remaining residue was triturated with diethyl ether (25 mL) with continues stirring for 30 minutes to afford a solid which was filtered, dried and crystallized from ethanol to give compounds **4a** or **4b** respectively.

*4-(4-phenyl-5-((3S,4R,5R)-3,4,5-trihydroxy-6-(hydroxymethyl)tetrahydro-2H-pyran-2-ylthio)-4H-1,2,4-triazol-3-yl)-1-(thiazol-2-yl)-3-(thiazol-2-ylamino)-1H-pyrrol-2(5H)-one***(4a)**:Yield: 70%; m.p.160-162^{o}C; IR (KBr) cm^{-1}, ν: 3240 (NH), 3354 (OH);^{1}H NMR (DMSO-d$_6$) δ/ppm: 3.39-3.46 (m, 2H, H-6′,6″), 3.62-3.65 (m, 1H, H-5′), 3.96-4.21 (m, 4H, N-CH$_2$, H-4′, H-3′), 4.42-4.47 (m, 1H, OH), 4.90-5.07 (m, 2H, OH and H-2′), 4.69- 4.73 (br, 2H, 2OH), 5.72 (d, 1H, J = 8.2 Hz, H-1′), 7.21 -7.34 (m, 4H, 2S-CH=, 2Ar-H); 7.45-7.74 (m, 5H, 2N-CH= and 3 Ar-H), 9.25(br, 1H, NH).^{13}C NMR (DMSO-d$_6$, δ ppm): 49.1 (CH$_2$), 58.3 (C-6′), 62.9 (C-4′), 67.5 (C-3′), 69.5 (C-2′), 73.7 (C-5′), 81.9 (C-1′), 88.7, 91.2, 96.6, 99.4, 113.5, 119.9, 124.2, 127.6, 130.1, 134.3, 139.2, 148.9, 152.1, 163.6 (thiazole-C, pyrrole-C, triazole-C), 164.5, 166.9, 173.2, 176.1, 178.3 (5C=O). Anal. Cald. For $C_{24}H_{23}N_7O_6S_3$ (601.09): C, 47.91; H, 3.85; N, 16.30. Found: C, 49.95; H, 3.87; N, 16.35 %.

4-(4-amino-5-((2R,3S,4R,5R)-3,4-dihydroxy-5-(hydroxymethyl)tetrahydrofuran-2-ylthio)-4H-1,2,4-triazol-3-yl)-1-(thiazol-2-yl)-3-(thiazol-2-ylamino)-1H-pyrrol-2(5H)-one **(4b)**: Yield: 63%; m.p. 205-207°C; IR (KBr) cm^{-1}, ν: 3220 (NH), 3460 (OH); ^{1}H NMR (DMSO-d_6) δ/ppm: 4.01-4.32 (m, 2H, N-CH_2, 4.39-4.44 (m, 2H, H-5′,5″), 4.51-4.60 (m, 4H, CH_2, H-4′,3′), 4.89-5.01 (m, 4H, NH_2, OH and H-2′), 5.12-5.22 (br,2H, 2OH), 5.84 (d, 1H, J = 9.4 Hz, H-1′), 6.89-7.05 (m, 2H, S-CH=); 7.31-7.52 (m, 2H, N-CH=), 9.22 (br, 1H, NH).[13] C NMR (DMSO-d_6, δ ppm) : 42.9 (CH_2), 45.8 (C-4′), 49.7 (C-3′), 56.7, (C-2′), 62.6 (C-5′), 69.1 (C-1′), 75.7, 89.2, 96.8, 112.5, 145.2, 155.3 (thiazole-C, pyrrole-C, triazole-C), 159.9, 161.1, 164.4, 170.5, 173.2 (5C=O). Anal. calcd. For $C_{17}H_{18}N_8O_5S_3$ (510.06): C, 39.99; H, 3.55; N, 21.95. Found: C, 40.02; H, 3.58; N, 21.99 %.

5.4.In-vitro anticancer activity:

5.4.1 Cell propagation and maintenance:

MCF-7 human breast cancer cells and HCT-116 human liver cancer cells were obtained from ATCC (American Type Culture Collection) and maintained in the proper conditions. The cells were cultured in Dulbecco's modified Eagle's Medium (DMEM) (Lonza, Belgium) supplemented by 10 % fetal bovine serum (FBS), 100 U/ml penicillin, and 100 µg/ml streptomycin sulfate at 37 ˚C in a humidified incubator with 5 % CO_2. The cells were harvested after trypsinization (0.025 % trypsin and 0.02 % EDTA) and washed twice with Dulbecco's phosphate-buffered saline (DPBS). When the cell density reached approximately 80%, cells were split for further culture. The experiments were made up when the cells were in the logarithmic growth phase.

5.4.2 Cytotoxicity assay:

Cell viability was measured by MTT (3-[4,5-dimethylthiazol-2-yl]-2,5 diphenyltetrazolium bromide) assay[47]. MTT assay is based on the conversion of MTT into formazan crystals by living cells, which reflects cytotoxicity based on mitochondrial activity[48]. The cytotoxic impact of the tested compounds measured by MTT assay using MCF-7 and HepG2 cells respectively. The cells were incubated with various concentrations of the test compounds (3.125,6.25, 12.5, 25µM) for 48 h at a cell density of 104 cells/well of 96 well plate. After 24h incubation, MTT dissolved in PBS was added to each well at a final concentration of 5 mg/ml, and the samples were incubated at 37ºC for 4 h. After 4 hours, the medium was decanted and dimethyl sulfoxide (DMSO) was added to each well and left for 30 minutes to dissolve formazan crystals that formed during MTT cleavage in actively metabolizing cells. The absorbance of formazan in each plate was measured at 570 nm, using a microplate reader (Model 500; BIORad Instrument Inc., USA). Using the relation between the used concentrations and the mitochondrial activity (%), the IC50 of the tested compound was calculated. For the untreated cells (negative control), the medium was added instead of the test compound. A positive control Doxorubicin (Dox, Mr= 543.5) was used as a cytotoxic natural agent giving 100% inhibition. Dimethyl sulfoxide (DMSO) was the vehicle used for dissolution of the tested compound and its final concentration on the cells was less than 0.2%. All tests and analyses were done in triplicate and the results were averaged. All the data are expressed as Mean ± SD. Data were calculated using Sigma plot ver. 125. Analysis of the data was done using a student t-test to detect the significant difference among the studied compounds. Differences were considered to be statistically significant when $P < 0.05$.

5.5. Molecular docking studies:

The molecular docking of novel compounds was fabricated using standard bond lengths and angles, with the MOE program and detected by Discovery Studio Client (version4.2)[22]. Following geometry optimization, a systematic conformational examination was supported out to an RMS gradient of 0.01 Å, with energy minimization of the resultant conformations employing the Confirmation Examination module implemented in Auto Dock Vina. crystallographic structure of the Ternary Complex of KRIT1 bound to both the Rap1 GTPase and the Heart of Glass (HEG1) cytoplasmic tail PDBID:(4hdq)[49] and Structural analysis of KSHV thymidylate synthase PDBID:5H38[50].Nine dispersed docking simulations were run via defaulting parameters and the confirmations were designated constructed on the arrangement of total statistics, E conformation, and appropriate with the relevant amino acids in the binding pocket for each protein, separately

5.6. Computational procedures:

Calculations of DFT with a hybrid functional B3LYP (Becke's three-parameter hybrid functional using the BLYP correlation functional) with the 6-311G(d) basis set using the Berny method[51], were performed with the Gaussian 09W program[28]. No symmetry constraints were applied during the geometry optimization. This method is often more accurate than those calculated with other approaches for the same basis set size and calculated the HOMO-

LUMO band gap energy, and physical descriptor's[26, 52, 53, 54].

Conclusion:

In this work, aminotriazole with bromogalactose and amination in the presence of ammonia solution were unique 1,2,4-triazole glycoside derivatives. In comparison to the reference medication doxorubicin, the derived triazole glycosides showed significant anti-proliferative activity against the human tumor cell lines HCT-116 and MCF-7. Additional research into their expected mode of accomplishment by analyzing molecular docking studies will give insight into the manner of binding and interactions of compounds 3a, 3b, 4a, and 4b with drug-binding proteins. PDB identifiers 5H38 and 4hdq demonstrated short bond distances and hydrogen bond interactions with various amino acids, as well as the stability of the chemicals in the protein's pocket. Furthermore, the B3LYP/6-31G basis sets explanation of compounds 3a, 3b, 4a, and 4b confirmed their stabilities because of their geometrical parameters, low energies, and stability. Additionally, the substituted 1,2,4- aminotriazole glycoside derivatives with the HOMO-LUMO gap symbolize stability and confirm the electron distribution to glycoside, increasing their reactivity in addition to the chemical reactivity for such compounds.

References:

[1] P. Franchetti, M. Grifantini, Nucleoside and non-nucleoside IMP dehydrogenase inhibitors as antitumor and antiviral agents, Current medicinal chemistry 6(7) (1999) 599-614.

[2] Y. Matsuya, T. Kawaguchi, K. Ishihara, K. Ahmed, Q.-L. Zhao, T. Kondo, H. Nemoto, Synthesis of macrosphelides with a thiazole side chain: New antitumor candidates having apoptosis-inducing property, J Organic Letters 8(20) (2006) 4609-4612.

[3] H. Tolan, M. Radwan, H. Khalaf, M. El-Bayaa, H. Awad, W. El-Sayed, Synthesis and Cytotoxic Activity of New 1, 4-Dithiazolyl-5-oxopyrrole Derivatives, Their 1, 2, 4-Triazoles and Nucleoside Analogs, Russian Journal of General Chemistry 90 (2020) 1544-1552.

[4] R. Lesyk, O. Vladzimirska, S. Holota, L. Zaprutko, A. Gzella, New 5-substituted thiazolo [3, 2-b][1, 2, 4] triazol-6-ones: Synthesis and anticancer evaluation, European journal of medicinal chemistry 42(5) (2007) 641-648.

[5] D. Kaminskyy, B. Zimenkovsky, R. Lesyk, Synthesis and in vitro anticancer activity of 2, 4-azolidinedione-acetic acids derivatives, European journal of medicinal chemistry 44(9) (2009) 3627-3636.

[6] H.E. Tolan, M.A. Radwan, H.A. Soliman, H.M. Awad, W.A. El-Sayed, Synthesis and Anti-Proliferative Activity of New Acridinyl and Benzothiazolyl-Based Triazole Glycosides via Click Cycloaddition and Their Tetrazolyl Analogs, Russian Journal of Bioorganic Chemistry 46 (2020) 1136-1147.

[7] H.E. Tolan, W.A. El-Sayed, N. Tawfek, F.M. Abdel-Megeid, O.M. Kutkat, Synthesis and anti-H5N1 virus activity of triazole-and oxadiazole-pyrimidine hybrids and their nucleoside analogs, Nucleosides, NucleotidesNucleic Acids 39(5) (2020) 649-670.

[8] M.A. Radwan, F.M. Alminderej, H.E. Tolan, H.M. Awad, Synthesis and Antiproliferative Activity of Chalcone-Imide Derivatives Based on 3, 4-Dichloro-1H-Pyrrole-2, 5-dione, Egyptian Journal of Chemistry 64(1) (2021) 1-9.

[9] I.S. Williams, P. Joshi, L. Gatchie, M. Sharma, N.K. Satti, R.A. Vishwakarma, B. Chaudhuri, S.B.J.B. Bharate, M.C. Letters, Synthesis and biological evaluation of pyrrole-based chalcones as CYP1 enzyme inhibitors, for possible prevention of cancer and overcoming cisplatin resistance, 27(16) (2017) 3683-3687.

[10] A.M. Fahim, H.E. Tolan, W.A. El-Sayed, Synthesis of novel 1, 2, 3-triazole based acridine and benzothiazole scaffold N-glycosides with anti-proliferative activity, docking studies, and comparative computational studies, Journal of Molecular Structure 1251 (2022) 131941.

[11] A.M. Farag, N.A. Kheder, A.M. Fahim, K.M. Dawood, Regioselective synthesis and computational calculation studies of some new pyrazolyl-pyridine and bipyridine derivatives, Journal of Heterocyclic Chemistry n/a(n/a) (2023).

[12] R. Whitley, C. Alford, F. Hess, R. Buchanan, Vidarabine: a preliminary review of its pharmacological properties and therapeutic use, Drugs 20 (1980) 267-282.

[13] J. Gallardo, B. Rubio, M. Fodor, L. Orlandi, M. Yanez, C. Gamargo, M. Ahumada, A phase II study of gemcitabine in gallbladder carcinoma, Annals of oncology 12(10) (2001) 1403-1406.

[14] F.N. El-Shall, A.M. Fahim, S. Dacrory, Making a new bromo-containing cellulosic dye with antibacterial properties for use on various fabrics using computational research, Scientific Reports 13(1) (2023) 10066.

[15] M.A. Shalaby, S.A. Rizk, A.M. Fahim, Synthesis, reactions and application of chalcones: a systematic review, Organic & Biomolecular Chemistry 21(26) (2023) 5317-5346.
[16] M.C. Walters III, F. Roe, A. Bugnicourt, M.J. Franklin, P.S. Stewart, Contributions of antibiotic penetration, oxygen limitation, and low metabolic activity to tolerance of Pseudomonas aeruginosa biofilms to ciprofloxacin and tobramycin, Antimicrobial agents

chemotherapy 47(1) (2003) 317-323.
[17] A.M. Fahim, E.H. Ismael, Theoretical Investigation of some Antimalarial Sulfonamides as COVID-19 Drug Utilizing Computational Calculations and Molecular Docking Study, Biointerface Research in Applied Chemistry 12(1) (2021) 1208-1229.
[18] A.M. Fahim, H.S. Magar, N.H. Mahmoud, Synthesis, antimicrobial, antitumor activity, docking simulation, theoretical studies, and electrochemical analysis of novel Cd(II), Co(II), Cu(II), and Fe(III) complexes containing barbituric moiety, Appllied Organomettalic Chemistry 37(4) (2023) e7023.
[19] H.E.M. Tolan, A.M. Fahim, E.H.I. Ismael, Synthesis, biological activities, molecular docking, theoretical calculations of some 1,3,4-oxadiazoles, 1,2,4-triazoles, and 1,2,4-triazolo[3,4-b]-1,3,4-thiadiazines derivatives, Journal of Molecular Structure 1283 (2023) 135238.
[20] A.M. Fahim, Anti-proliferative activity, molecular docking study of novel synthesized ethoxyphenylbenzene sulfonamide with computational calculations, Journal of Molecular Structure 1277 (2023) 134871.
[21] A.M. Fahim, H.E. Tolan, H. Awad, E.H. Ismael, Synthesis, antimicrobial and antiproliferative activities, molecular docking, and computational studies of novel heterocycles, Journal of the Iranian Chemical Society 18(11) (2021) 2965-2981.
[22] S. Vilar, G. Cozza, S. Moro, Medicinal chemistry and the molecular operating environment (MOE): application of QSAR and molecular docking to drug discovery, Current topics in medicinal chemistry 8(18) (2008) 1555-1572.
[23] G.H. Elsayed, A.M. Fahim, A.I. Khodair, Synthesis, anti-cancer activity, gene expression and docking stimulation of 2-thioxoimidazolidin-4-one derivatives, Journal of Molecular Structure 1265 (2022) 133401.
[24] A. Fahim, E. Ismael, Synthesis, antimicrobial activity and quantum calculations of novel sulphonamide derivatives, Egyptian Journal of Chemistry 62(8) (2019) 1427-1440.
[25] A.M. Fahim, M.A. Shalaby, Synthesis, biological evaluation, molecular docking and DFT calculations of novel benzenesulfonamide derivatives, Journal of Molecular Structure 1176 (2019) 408-421.
[26] A. Aboelnaga, E. Mansour, A.M. Fahim, G.H. Elsayed, Synthesis, anti-proliferative activity, gene expression, docking and DFT investigation of novel pyrazol-1-yl-thiazol-4 (5H)-one derivatives, Journal of Molecular Structure 1251 (2022) 131945.
[27] A.M. Fahim, H.S. Magar, N.H. Mahmoud, Synthesis, anti- proliferative activities, docking studies, and computational calculations of novel isonicotinic mixed complexes, Applied Organometallic Chemistry 36(5) (2022) e6616.
[28] A. Frisch, gaussian 09W Reference, Wallingford, USA, 25p (2009).
[29] H. Bayrak, A.M. Fahim, F. Yaylaci Karahalil, I. Azafad, G.M. Boyraci, E. Taflan, Synthesis, antioxidant activity, docking simulation, and computational investigation of novel heterocyclic compounds and Schiff bases from picric acid, Journal of Molecular Structure 1281 (2023) 135184.
[30] A. Attia, A. Aboelnaga, A.M. Fahim, ISONICOTINOHYDRAZIDE CHALCONE BASE AND ITS Ni COMPLEX AS CORROSION INHIBITORS DURING ACID CLEANING: THEORETICAL AND EXPERIMENTAL APPROACHES, Egyptian Journal of Chemistry (2022).
[31] P.K. Chattaraj, A. Cedillo, R.G. Parr, Chemical softness in model electronic systems: dependence on temperature and chemical potential, Chemical physics 204(2-3) (1996) 429-437.
[32] W. Gordy, W.O. Thomas, Electronegativities of the elements, The Journal of Chemical Physics 24(2) (1956) 439-444.
[33] A. Hanna, M. Tinkham, Variation of the Coulomb staircase in a two-junction system by fractional electron charge, Physical review B 44(11) (1991) 5919.
[34] R.G. Parr, R.G. Pearson, Absolute hardness: companion parameter to absolute electronegativity, Journal of the American chemical society 105(26) (1983) 7512-7516.
[35] L.R. Domingo, M.J. Aurell, P. Pérez, R. Contreras, Quantitative characterization of the global electrophilicity power of common

diene/dienophile pairs in Diels–Alder reactions, Tetrahedron 58(22) (2002) 4417-4423.
[36] A. Vela, J.L. Gazquez, A relationship between the static dipole polarizability, the global softness, and the fukui function, Journal of the American Chemical Society 112(4) (1990) 1490-1492.
[37] A. Ino, T. Mizokawa, A. Fujimori, K. Tamasaku, H. Eisaki, S. Uchida, T. Kimura, T. Sasagawa, K. Kishio, Chemical potential shift in overdoped and underdoped La 2− x Sr x CuO 4, Physical review letters 79(11) (1997) 2101.
[38] M.A. Shalaby, A.M. Fahim, S.A. Rizk, Microwave-assisted synthesis, antioxidant activity, docking simulation, and DFT analysis of different heterocyclic compounds, Scientific Reports 13(1) (2023) 4999.
[39] A.M. Fahim, M.A. Shalaby, M.A. Ibrahim, Microwave-assisted synthesis of novel 5-aminouracil-based compound with DFT calculations, Journal of Molecular Structure 1194 (2019) 211-226.
[40] A.M. Fahim, A.M. Farag, G.A. Nawwar, E.S.M. Yakout, E.A. Ragab, Synthesis and DFT calculations of aza-Michael adducts obtained from degradation poly (methyl methacrylate) plastic wastes, International Journal of EnvironmentWaste Management 24(4) (2019) 337-353.
[41] A.M. Fahim, A. Farag, E. Yakout, G. Nawwar, E. Ragab, Synthesis, biological evaluation of 1, 3, 4-oxadiazole, triazole and uracil derivatives from poly (ethylene terephthalate) waste, Egypt. J. Chem 59(3) (2016) 285-303.
[42] A.M. Fahim, M.S. Elshikh, N.M. Darwish, Synthesis, antitumor activity, molecular docking and DFT study of novel pyrimidiopyrazole derivatives, Current computer-aided drug design 16(4) (2020) 486-499.
[43] A.M. Fahim, E.E. Abu-El Magd, Performance efficiency of MIP OH polymers as organic filler on cellulose pulp waste to form cellulosic paper sheets with biological evaluation and computational studies, Polymer Bulletin (2021) 1-33.
[44] M.A. Shalaby, A.M. Fahim, S.A. Rizk, Antioxidant activity of novel nitrogen scaffold with docking investigation and correlation of DFT stimulation, RSC Advances 13(21) (2023) 14580-14593.
[45] A.M. Fahim, M. Hasanin, I.H.I. Habib, R.O. El-Attar, S. Dacrory, Synthesis, antimicrobial activity, theoretical investigation, and electrochemical studies of cellulosic metal complexes, Journal of the Iranian Chemical Society (2023).
[46] E.A. Gendy, A.I. Khodair, A.M. Fahim, D.T. Oyekunle, Z. Chen, Synthesis, characterization, antibacterial activities, molecular docking, and computational investigation of novel imine-linked covalent organic framework, Journal of Molecular Liquids 358 (2022) 119191.
[47] H. Wang, H. Cheng, F. Wang, D. Wei, X. Wang, An improved 3-(4, 5-dimethylthiazol-2-yl)-2, 5-diphenyl tetrazolium bromide (MTT) reduction assay for evaluating the viability of Escherichia coli cells, Journal of microbiological methods 82(3) (2010) 330-333.
[48] A. Van Tonder, A.M. Joubert, A.D. Cromarty, Limitations of the 3-(4, 5-dimethylthiazol-2-yl)-2, 5-diphenyl-2H-tetrazolium bromide (MTT) assay when compared to three commonly used cell enumeration assays, BMC research notes 8 (2015) 1-10.
[49] A.R. Gingras, W. Puzon-McLaughlin, M.H. Ginsberg, The structure of the ternary complex of Krev interaction trapped 1 (KRIT1) bound to both the Rap1 GTPase and the heart of glass (HEG1) cytoplasmic tail, Journal of Biological Chemistry 288(33) (2013) 23639-23649.
[50] Y.M. Choi, H.K. Yeo, Y.W. Park, J.Y. Lee, Structural analysis of thymidylate synthase from Kaposi's sarcoma-associated herpesvirus with the anticancer drug raltitrexed, PloS one 11(12) (2016) e0168019.
[51] Y.V. Suleimanov, W.H. Green, Automated discovery of elementary chemical reaction steps using freezing string and Berny optimization methods, Journal of chemical theory and computation 11(9) (2015) 4248-4259.
[52] A.M. Fahim, A.M. Farag, A. Mermer, H. Bayrak, Y. Şirin, Synthesis of novel β-lactams: Antioxidant activity, acetylcholinesterase inhibition and computational studies, Journal of Molecular Structure 1233 (2021) 130092.
[53] A.M. Fahim, A.M. Farag, E.S.M. Yakout, G.A. Nawwar, E.A. Ragab, Sun degradation and synthesis of new antimicrobial and antioxidant utilising poly (ethylene terephthalate) waste, International Journal of EnvironmentWaste Management 22(1-4) (2018) 239-259.
[54] A.M.Fahim, E.H.I.Ismael, H.E.M.Tolan; Numerous Heterocyclic Compounds with an Isonicotinic Moiety have Been Studied for Their Synthesis, Antibacterial, Anticancer, Docking Simulation, and DFT Characteristics;Polycyclic Aromatic Compounds(2023), DOI: 10.1080/10406638.2023.2266549.